13 (2022) 100073

Contents lists available at ScienceDirect

Journal of Non-Crystalline Solids: X

journal homepage: www.sciencedirect.com/journal/journal-of-non-crystalline-solids-x

Decoupling polymer, water and ion transport dynamics in ion-selective membranes for fuel cell applications☆

Fabrizia Foglia [a,*], Victoria Garcia Sakai [b], Sandrine Lyonnard [c], Paul F. McMillan [a]

[a] Dept. of Chemistry, Christopher Ingold Laboratory, University College London, 20 Gordon St., London WC1H 0AJ, UK
[b] ISIS Neutron and Muon Source, Rutherford Appleton Laboratory, Harwell Science and Innovation Campus, Chilton OX11 0QX, UK
[c] Université Grenoble Alpes, CNRS, CEA, IRIG-SyMMES, 38000 Grenoble, France

ARTICLE INFO

Keywords:
Neutron
PEM
AEM

ABSTRACT

Ion conducting polymer membranes are designed for applications ranging from separation and dialysis, to energy conversion and storage technologies. A key application is in fuel cells, where the semi-permeable polymer membrane plays several roles. In a fuel cell, electrical power is generated from the electrochemical reaction between oxygen and hydrogen, catalysed by metal nanoparticles at the cathode and anode sites. The polymer membrane permits the selective transport of H^+ or OH^- to enable completion of the electrode half-reactions, plays a major role in the management of water that is necessary for the conduction process and is a product in the reactions, and provides a physical barrier against leakage across the cell. All of these functions must be optimised to enable high conduction efficiency under operational conditions, including high temperatures and aggressive chemical environments, while ensuring a long lifetime of the fuel cell. Polymer electrolyte membranes used in current devices only partially meet these stringent requirements, with ongoing research to assess and develop improved membranes for a more efficient operation and to help realise the transition to a hydrogen-fuelled energy economy. A key fundamental issue to achieving these goals is the need to understand and control the nature of the strongly coupled dynamical processes involving the polymer, water and ions, and their relationship to the conductivity, as a function of temperature and other environmental conditions. This can be achieved by using techniques that give access to information across a wide range of timescales. Given the complexity of the dynamical map in these systems, unravelling and disentangling the various processes involved can be accessed by applying the "serial decoupling" approach introduced by Angell and *co*-workers for ion-conducting glasses and polymers. Here we introduce this concept and propose how it can be applied to proton- and anion-conducting fuel cell membranes using two main classes of these materials as examples.

1. Introduction

Semi-permeable membranes designed to conduct specific ions are essential components of devices for energy conversion and storage, hydrogen production, water purification, dialysis and other separation technologies. They are central to the operation of fuel cells (FC) that employ electrocatalytic oxidation-reduction reactions of H_2 and O_2 to generate H^+ or OH^- ions at the cathode and anode sites. These ions are then transported via polymer-electrolyte membranes (PEM) to form H_2O at the opposing electrode, while the electrons released in the electrochemical reaction travel through an external circuit providing electrical power. Redox flow batteries employ reverse osmosis (RO) through ion-selective membranes to store electrical charge, and emerging energy-related technologies involve transport of Na^+ and other species through an ion-selective polymer or gel membrane. In all these cases, the ion transport is strongly coupled to nanoconfined or mobile H_2O species included within the membrane, as well as to the polymer segmental, main chain and side chain dynamics. It is critically important to understand and characterise these various processes and the dynamical interplay between them as a function of temperature, hydration state and other operational parameters in order to optimize and design next generation membranes for fuel cells and related energy applications.

The processes involved are studied using complementary experimental tools that probe the dynamics over a wide range of time- and

☆ Part of a special issue of Journal of Non-Crystalline Solids dedicated to honour the contributions of C. Austen Angell

* Corresponding author.
E-mail address: f.foglia@ucl.ac.uk (F. Foglia).

https://doi.org/10.1016/j.nocx.2021.100073
Received 28 September 2021; Received in revised form 30 November 2021; Accepted 2 December 2021
Available online 8 December 2021

distance scales, in combination with advanced simulation studies [1,2]. The results are expressed in terms of relaxation maps that help reveal and disentangle the characteristic timescales of different dynamic processes similar to those studied in other more general material classes such as glasses, polymers and glass-forming liquids, as a function of temperature, pressure or other environmental conditions. The examination of such maps led Austen Angell to develop the serial decoupling concept for ion-conducting glasses, which was extended to ion-matrix systems in polymer electrolytes. In this model, the ionic conductivity becomes decoupled from the primary mechanical relaxation of the polymer framework and continues with approximately Arrhenius behaviour below the glass transition temperature, T_g [3–7]. Principles developed by Angell and his *co*-workers have been applied to analyze the multi-timescale dynamics associated with the strongly coupled polymer, water and ion conduction dynamics in PEM fuel cells [8,9]. Here, we show how the approach can be extended to examine and disentangle the complex coupled interactions between relaxation and diffusional phenomena in proton- and anion-conducting membranes for fuel cells and related applications as a function of their relative timescales, to provide useful insights into the ionic transport and water management mechanisms. We illustrate our discussion with recent examples studied as a function of temperature and membrane hydration levels.

2. Time-temperature dependence of relaxation processes in non-polymeric glass-forming systems

In order to introduce the relative timescales of different mechanical or enthalpic relaxation processes, we begin by considering the glass transition in inorganic systems.

In the liquid state, the rate of dissipation of mechanical strain (ε) due to cooperative structural configurational rearrangements, is rapid compared with typical observational timescales. The rate of strain removal ($\dot{\varepsilon}$) from the system determines the (shear) viscosity (η_s), that is linked to relaxation timescale (τ) by G_∞/η_s. G_∞ is the intrinsic mechanical resistance at long ("infinite") timescales, $\sim 10^{10}$ Pa for most glass-forming liquids. Plotting the logarithm of liquid viscosity as a function of inverse temperature usefully scaled by the glass transition (T_g), provides a set of comparable relationships that range from approximately linear (Arrhenius) to strongly curved behaviour that is typically described using a Vogel-Tammann-Fulcher (VTF) relationship. In 1991, Angell discussed such log η_s vs T_g/T patterns for a wide range of liquids to define a gradation between "strong" (i.e. highly Arrhenian) to "fragile" behaviour [10]. When η_s is determined under laboratory conditions, the stress is applied and the strain relaxation is observed over a period $\sim 10^2$ s, leading to a viscosity of $\sim 10^{12}$ Pa.s at T_g, the point at which the mechanical strain inside the material is no longer relaxed on the observational timescale, so that it is said to behave as a rigid amorphous or glassy solid.

The glass transition is also typically recorded by calorimetric measurements as an endothermic signal appearing in differential scanning calorimeter (DSC) traces. The rate of enthalpy evacuation from the material is typically approximately correlated with that of mechanical strain relaxation, although the "mechanical" and "calorimetric" T_g values can differ by up to an order of magnitude for highly fragile glass forming systems, and they can lead to different interpretations of the meaning of the glass transition event [10]. The onset of mechanical rigidity that marks the passage of the system from relaxed ("liquid") to unrelaxed ("glassy") behaviour is known as the primary or "α" relaxation. Below T_g, the primary means of structural equilibration are no longer available to the system, but other modes of configurational relaxation may still remain active within the glassy solid. Such secondary or "β" relaxational processes may include diffusion of ions or molecular species through the matrix, and local structural excursions such as molecular rotational degrees of freedom [10]. All of these dynamic configurational changes are strongly coupled to each other in the liquid state. Below the glass transition, some degree of coupling remains, until each β relaxation with its own characteristic activation energy and timescale becomes successively "frozen" as the temperature is lowered.

The "decoupling index" first described by Angell in 1983 was used to describe how well the ionic transport modes became decoupled from the amorphous matrix, in fast ion-conducting glasses [3]. Torell and Angell then extended the concept to polymer electrolyte systems, where they applied the decoupling concept and index to describe and quantify how the α and β relaxations associated with polymer main and side chain dynamics become serially uncoupled from configurational changes in the solvation shells around the ions and the fast ion conduction mechanism [4]. These are important design concepts in the field of glassy and polymeric materials exhibiting superionic conduction [5–7], as well as for understanding the properties of ionic and molecular liquids [11,12]. They also highlight important fundamental questions that continue to exercise the various communities concerned with glassy, liquid and polymer dynamics [13,14]. We incorporate them here along with the dynamical processes encountered among polymeric systems in our extension of the discussion to ion conducting membranes.

3. Relaxation dynamics in ion conducting polymeric membranes

The mechanical and sub-T_g relaxations in polymeric systems are inherently more complex and subtle to interpret than those in ionic or molecular glass-forming liquids. In ion-conducting polymers, these local and segmental structural relaxation processes are strongly coupled to the ionic conduction mechanisms, especially at high temperature. As the temperature is decreased, the highly non-Arrhenian polymer dynamics diverge from the ionic conduction that continues with an Arrhenian temperature dependence, and analysis of this divergence forms the basis of the "serial decoupling" phenomena first described by Angell. In the case of H^+ or OH^- conducting ionomers used in fuel cells, incorporated water plays a key role in the ion transport mechanism, and so the problem becomes even more complex, requiring the analysis of coupled polymer dynamics, diffusion and relaxation dynamics of bulk and nanoconfined H_2O, and ionic conduction. Using a combination of techniques to analyze these coupled contributions to the relaxation and diffusional dynamics over a wide range of time- and distance scales, as a function of temperature, pH and membrane hydration state, provides a useful approach for deciphering the membrane function and performance.

Relaxations in polymers include those arising from the main chain, those from localized regions (segments) that relax independently but are always strongly correlated with the main chain motions, and those from polymer side chains and functional groups (e.g. pseudo-rotational modes of methyl groups about the C-CH_3 bond axis, or side groups associated with ionic behaviour). For this reason, the relaxation map of polymer systems is significantly more complicated than for molecular systems. In the high temperature liquid state the main chain and segmental dynamics occur on similar timescales that slow down according to stretched exponential kinetics. The primary α relaxation related to the glass transition typically recorded by a principal DSC endotherm, occurs when the timescale of the segmental dynamics reaches $\sim 10^2$ s. In the fully molten state the other dynamic processes are also detected with faster relaxation timescales. The secondary or β relaxations, which follow an approximately Arrhenius behaviour (in log τ vs $1/T$) begin to diverge from the main chain and segmental relaxations just above T_g. Finally, other faster relaxations including methyl group rotations maintain an independent signature to very high temperature, where all processes converge near the vibrational timescale of $\tau \sim 10^{-12}$ s. As the system is cooled below T_g it typically enters a rubbery state, in which it no longer flows in a liquid like manner but is highly flexible and deformable, generally returning to a close approximation of its original form on removal of applied stress [15,16]. Finally, at some lower temperature the system becomes fully rigid exhibiting brittle solid-like or glassy behaviour, as secondary relaxation dynamics become de-

activated so the polymer can no longer readjust its shape in response to the applied stress field on the observational timescale. For ion-conducting polymers, the ionic conduction is closely coupled to the segmental, main chain and side group dynamics, making it essential to understand the relaxation map in these systems. In polymeric membranes designed and implemented to transport H^+ ions in proton-conducting PEM systems, as well as in anion (OH^-) conducting AEMFCs, the transport dynamics rely on mediation by sulphonate (OSO_3^-) or other charged side groups attached to the polymer chain to mediate the proton transfer reactions, as well as H_2O molecules contained within the membrane that mediate the proton transfer or OH^- diffusion processes. These add further elements to the complex dynamical map, as one needs to understand the role of the diffusion of confined H_2O and H^+/OH^- transport processes. Thus it becomes essential to study and understand the degree and nature of the coupling between the polymer, H_2O and ion dynamics with conductivity as a function of temperature and membrane hydration state, in order to optimize and design PEM systems for efficient fuel cell operation.

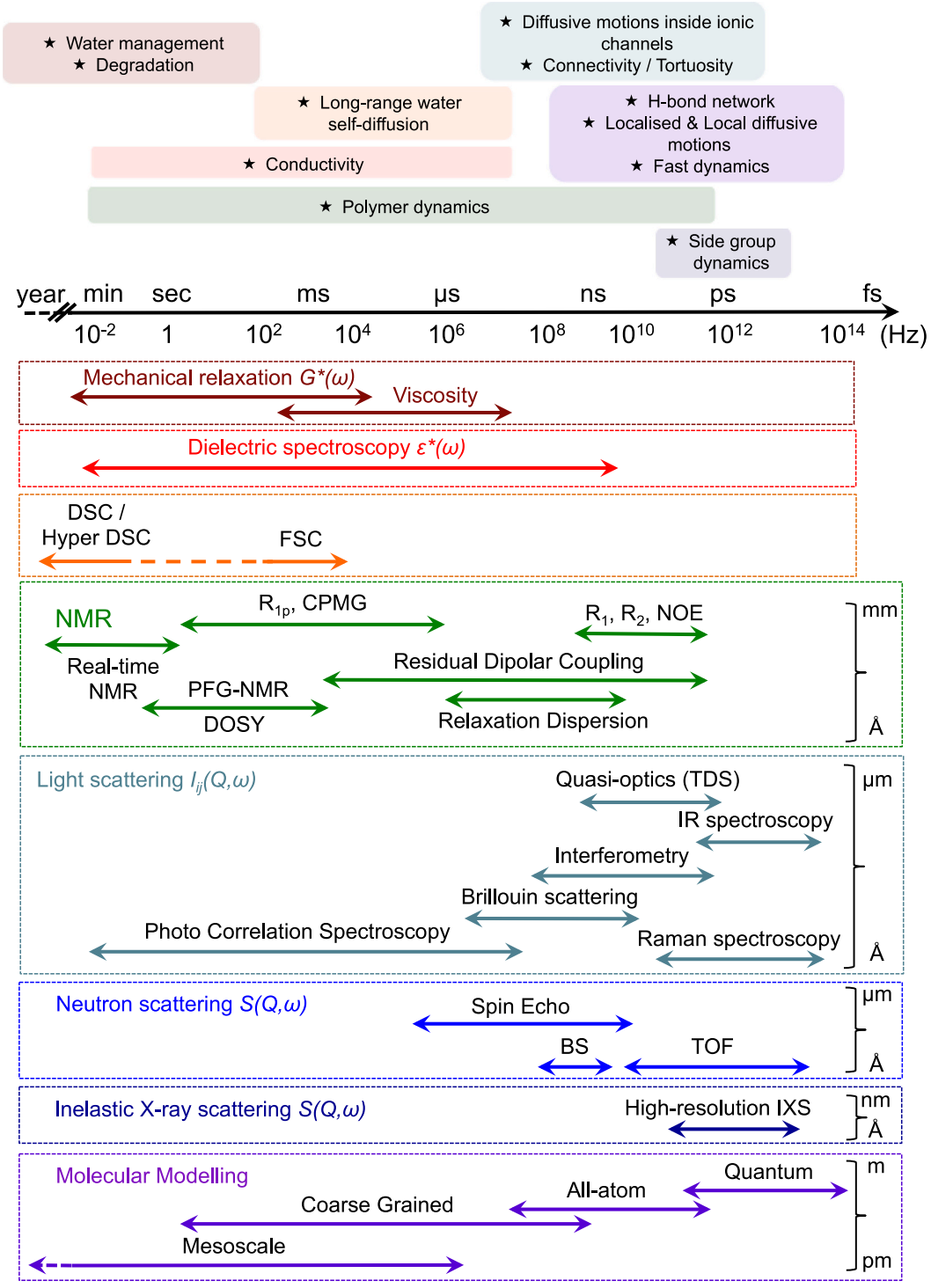

Fig. 1. Comparative illustration of the frequency (time) and length scale ranges accessible with a range of different techniques. Timescale data ranges taken from refences [1,34–36].

The membrane of choice for proton conducting PEMFCs is currently one of a class of perfluorocarbon sulfonic acid (PFSA) polymers known as "Nafion®". These incorporate sulfonate groups attached to the polymer side chain that enable rapid conduction of protons through a hydrogen-bonded system that involves H_2O molecules. Such PEMFC devices typically operate at ~80 °C. To allow more efficient operation at higher temperatures (up to 200 °C) especially for automotive systems will require design of new membrane systems aided by advances in fuel cell technology [18–20]. One key consideration is the glass transition temperature, ~130 °C for dry Nafion, which decreases rapidly as a function of membrane water content, ~108 °C at 24% hydration [21–23]. The coupling between polymer, water and ion transport dynamics is expected to show fundamental changes as the operating temperature is raised throughout the 100–200 °C region. The situation is even less clear for anion-conducting membranes, which could supplant the use of Pt-based electrocatalysts by using first row transition metals such as Ni and Co [24]. However, developing membrane materials that exhibit sufficiently efficient conduction while withstanding the extremely alkaline conditions required for operation constitutes an active area of research [25–27]. Both Grotthuss hopping of H^+ ions and vehicular OH^- transport mechanisms are implicated in the conduction process of anion exchange membranes (AEM), with the balance between them depending on the hydration state of the membrane [28–32]. Deciphering the complex nature of the charge transport process with its multiply coupled elements of polymer main- and side-chain dynamics, H_2O as both a facilitator of ion exchange and H^+/OH^- conduction and as a diffusive species in its own right, represents a major challenge that must be addressed for optimal AEMFC design and implementation. One such way forward is to apply the principles of Angell's serial decoupling approach to relaxational/diffusional modes from data obtained over multiple time- and length-scales.

4. Methods to probe relaxation maps for PEMFCs

Multiple techniques are employed to study glass forming liquids and polymeric systems, providing information on the relaxation dynamics across wide ranges of timescales and correlation lengths (Fig. 1). Common laboratory techniques such as IR and Raman spectroscopies are used alongside large scale X-ray and neutron scattering at national and international facilities to investigate the structure of such systems, as a function of temperature, processing and environmental conditions. Although these techniques are typically applied to obtain averaged information on bulk samples, mapping experiments can also be carried out especially using the latter two to study spatially-resolved structures and processes within samples including under operando conditions. In terms of dynamical features, processes in the hours to ms timescales can be probed by mechanical measurements, dielectric spectroscopy, light scattering or nuclear magnetic resonance (NMR) spectroscopy. For the faster processes, neutron scattering methods offer very detailed complementary information to these techniques, accessing dynamics in the 10^{-9}–10^{-14} s range.

The ability to disentangle processes such as polymer dynamics, ion hopping, and water trapped within the matrix is crucial to optimize membrane and device performance under operational conditions. For example, in the case of PEMFCs the ability to control water dynamics is critical to optimize proton exchange performance while preventing phenomena such as membrane drying and/or electrode flooding [33]. Neutron scattering (NS) is one of the most powerful tools available to highlight and disentangle these complex cooperative process dynamics as a function of their characteristic timescales. In addition, because of the deep penetration of neutron beams into matter including experimental cell enclosures, NS experiments readily permit in situ and operando studies in sample environments that correspond to or mimic actual devices, providing a unique view into the interplay between structure and dynamics under operational conditions.

Differential scanning calorimetry (DSC) is typically used to examine the thermal relaxation properties of materials including polymers. Here the sample is heated or cooled at a specified rate and heat flow into or out of the system recorded as an *endo*- or exothermic event. As a polymeric liquid is cooled metastably below its normal crystallization point, the main endotherm corresponds to the α process, that is associated with the inability of the segmental relaxation dynamics to achieve equilibration on the timescale of calorimetric experiment. This T_g temperature varies with the cooling rate applied to the sample, and on re-heating samples initially quenched into a solid amorphous state or having undergone subsequent thermal or mechanical processing, a different value can be recorded during re-heating [37]. At lower temperature, one or more subsidiary endotherms are typically observed, that are designated as "β" relaxations. These are often assigned to sub-T_g relaxation processes including side-chain dynamics, but have also been ascribed to formation of nanocrystalline domains within the amorphous polymer [38–41]. Mechanical relaxation dynamics are investigated by viscosity measurements in the stable and supercooled liquid state, and also by indentation, bending or other techniques designed to explore either the kinetics of initial formation of an initial strained state or return of the system to its initial geometry following an applied stress. These studies are critically important to examine the mechanical behaviour of polymers used in FCs and for other separation technologies, as these materials encounter variable temperatures, internal stresses due to incorporation of water, and other environmental conditions during operation.

NMR spectroscopy is widely used to obtain information on the kinetics of ionic and molecular diffusion, reorientation and chemical reactions and the coupling between them. Different NMR techniques allow probing events on timescales ranging from the picosecond to millisecond regime, and even longer. A first set of timescales is introduced by the coupling between nuclei in different chemical environments, where the coalescence between individual peaks or multiplet splittings as a function of temperature or other chemical and physical conditions gives access to a timescale represented by the peak separation in s^{-1}. These depend on the gyromagnetic ratio, spin quantum number of the nuclei involved at a particular magnetic field, and the strength of the coupling between the different nuclei. In this way, the temperature dependence of motional averaging of the different nuclei and chemical environments gives access to timescales extending throughout the μs-ms range. Studying different NMR relaxation times using multiple pulse techniques probes a much wider range of timescales extending between approximately 10^{-8} and 10^{-10} s, that are caused by local fluctuations in the magnetic dipolar and electric quadrupolar properties due to electromagnetic interactions in the nuclear environments [42]. This timescale range is constantly being expanded as new instrumentation and pulse sequences are developed and applied to probe the relaxation events [43]. NMR experiments are often performed to study water and ion diffusion in polymer/ionomer membranes and other nanoporous materials using static or pulsed field gradients, to gain access to timescales that overlap those of molecular diffusion and conductivity studies [44–48]. The majority of these NMR techniques typically provide information on dynamic relaxation processes occurring over a molecular scale, averaged across the entire sample. Experiments in a magnetic field gradient allow access to dynamics on a timescale of several tens of ms and distances on the order of a few hundred nm to several μm, which is relevant to membrane operation [47–51]. Pulsed field gradient, diffusion-oriented NMR spectroscopy utilizes spatially-dependent pulsed magnetic field gradients to directly quantify diffusion coefficients for species containing protons and other NMR-active nuclei over ms timescales. NMR relaxometry probes the relaxation rate (inverse of T_1) over an extended range of frequency, providing insights into the local dynamics typically in the range of microseconds [52–54]. Furthermore, magnetic resonance imaging (MRI), mainly applied to study time- and spatially-resolved proton concentrations and diffusional processes, is used to observe the T_1 or T_2 relaxation times of ^1H nuclei attached to H_2O or as H^+/OH^- species located at various positions

within or diffusing through the membrane. Profiles are established over a timescale of seconds to minutes, at a spatial resolution of a few μm, and such studies have been carried out for PEMFCs under operational working conditions [55–57].

Because the ionic conduction processes involve movement of charged species, they are examined by AC conductivity and time-resolved analysis of the electrical impedance properties, probing timescales extending between 10^{-15} to 10^{5} s associated with processes ranging from electronic and ionic polarization to hopping and space charge polarization dynamics. The data produced by these investigations can be combined into a single plot as a function of the different timescales of the cooperatively interacting relaxation or diffusional processes, in order to disentangle their contributions to the dynamics.

Neutron scattering spectroscopy, in particular the technique of Quasi Elastic Neutron Scattering (QENS), provides a direct measurement of the relative displacement of all atoms and molecular groupings within the sample. In particular, since the so-called *incoherent scattering* (that provides a measure of the interaction between the neutron and atomic nuclei) from H atoms is so much greater than that of all other elements, it probes the displacement of hydrogen atoms and hydrogen-containing species in a sample. In this sense, QENS allows a unique perspective on where the H-atoms are located relative to each other and how they move, on a timescale that ranges from sub-ps to hundreds of ns. In practical terms, each relaxation process gives rise to a QENS profile that corresponds to a broadening in the energy transfer function ($\pm \Delta\hbar\omega$, modelled as a Lorentzian process) around an elastic signal ($\delta(\omega)$). The scattering profile is described in terms of a dynamical structure factor, $S(Q,\omega)$ or its Fourier transform ($I(Q,t)$, where Q is the momentum transfer), as illustrated in Fig. 2.

In the energy domain, QENS data are typically described by the examining the dependence of the Lorentzian linewidth (Γ = half-width at half-maximum; HWHM) with respect to Q^2. The resulting relationship can be dispersive, corresponding to diffusive dynamics, or *non-dispersive*, associated with localized dynamics (e.g., polymer segmental relaxation, reorientation/rotation motions, etc.). In the case of localized motions, a characteristic relaxation time (τ) is given by $\Gamma = 1/\tau$. For dispersive behaviour, on the other hand, examining the $\Gamma(Q^2)$ relations permits evaluation of the self-diffusion coefficient (D) of the moving particle. Theoretically, for Fickian diffusion, Γ follows the DQ^2 law. However, this is only valid at low-Q values ($\leq$0.1 Å^{-1}). At higher Q the Γ vs Q^2 behaviour reveals instead a detailed view of short-range proton dynamics, by fitting the data to so-called "jump" or "rattle and hop" models, at various degrees of model sophistication [58–59]. Information gained from QENS is highly complementary to that obtained from pulsed field gradient (PFG-) NMR [35,60–63], with the additional advantages that it provides spatial information for the diffusion process, and it allows one to obtain information on dynamics of confined species at the nanoscale. In this particular case, the Γ vs Q^2 plot is characterised by a plateau occurring at low-Q (Γ_0), before the onset of jump-diffusion behaviour. From analysis of the plateau in reciprocal space and time dimensions, it is possible to extract information about the local diffusion coefficient within the confinement region (D_{loc}), as well as the radius (a) of the confining area according to: $\Gamma_0 = 4.33\, D_{loc}/a^2$ [64–66].

In order to disentangle the dynamic contributions of different species or parts of the complex study under investigation with QENS, it is typically necessary to employ a range of different spectrometers that access different timescales, often at different neutron scattering instruments and facilities (that may be worldwide), while taking advantage of the unique contrast variation available to NS studies due to widely different incoherent scattering cross-section for ^{1}H (80.26 barns) ^{2}H (D: 2.05 barns). In this way, selective deuteration allows highlighting the dynamics of specific parts of the system under study. This approach is particularly efficient when the dynamics to be disentangled are associated with two different components, e.g., water and polymer species. However, when the dynamical processes to be distinguished arise from a single component (e.g. polymer α- vs β-relaxations) and/or the system under investigation is characterised by multimodal dynamics, the best approach is to combine data from several neutron spectrometers that cover the wide range of timescales associated with the relevant processes (Table 1).

One example is shown in Fig. 3 for the case of a polymer membrane hydrated in liquid/vapour water. Fig. 3a shows the profile taken on a given neutron spectrometer and the result of fitting the data to two Lorentzian functions centred at E = 0 (blue and green curves), with one corresponding to the polymer dynamics and the second to the diffusion of water molecules. Other atoms present within the system move on timescales slower than those that can be accessed by the spectrometer, so that their dynamics are subsumed into the so-called elastic line, which is modelled as a delta function convoluted with the instrumental resolution function (grey curve in Fig. 3a,b). The overall scattering function can be expressed as:

$$S(Q,\omega) = \{\delta(\omega)\,\Phi_{immobile} + (1-\Phi_{immobile})[x_1 S_P(Q,\omega) + (1-x_1)\,S_W(Q,\omega)]\} \bigotimes R(\omega) \quad (1)$$

where S_P and S_W are the scattering functions for polymer and water respectively, $\Phi_{immobile}$ is the fraction of "immobile" atoms (relative to the probe timescale used), and $R(\omega)$ is the instrumental resolution function, typically determined by acquiring the scattering profile of either a Vanadium standard, or from a QENS measurement of the sample at very low temperatures (~2–10 K), where only vibrational dynamics are presumed to be present. We note that the scattering function contains an implicit "resolution effect", which translates into specific dynamics being "visible or not" within the time-scale accessible by a specific instrument. This effect can be accounted for by considering the scattering law in the time domain, in which each contribution is normalised according to its relevant resolution function. The scattering expression becomes:

$$I(Q,t) = x_1\, I_P(Q,t) + (1-x_1)\left[N_{slow} I_{W_{slow}}(Q,t) + N_{fast} I_{W_{fast}}(Q,t)\right] \quad (2)$$

where $I(Q,t)$ is the so-called intermediate scattering function, and I_P and

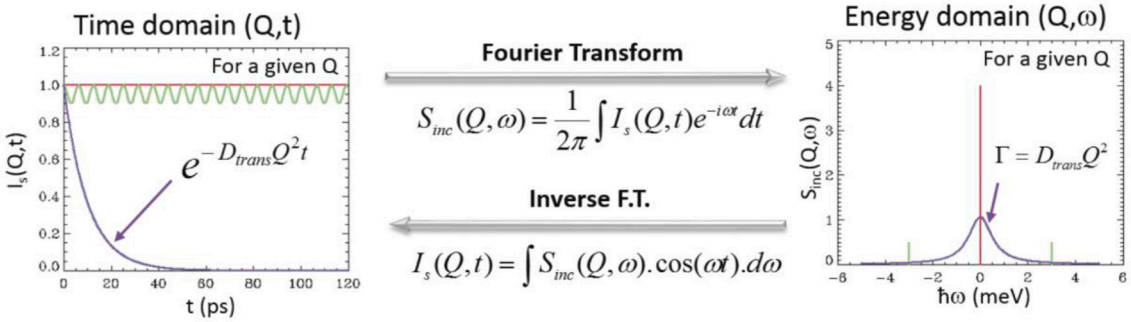

Fig. 2. Schematic representation of the typical data profile obtained in QENS for a single relaxation process. Reprinted with permission from [35].

Table 1
Beam-lines suitable for QENS studies at different neutron scattering facilities, with their achievable energy resolution (E_{res}) and Q range, as well as accessible timescale and detectable dynamics. ISIS (Neutron and Muon Spallation source; United Kingdom); ILL reactor source (Institut Laue-Langevin; France); FRM-II (Research Neutron Source Heinz Maier-Leibnitz; Germany); PSI (Paul Scherrer Institute, SINQ; Switzerland); SNS (ORNL, Oak Ridge National Laboratory Spallation Neutron Source; USA); NIST (National Institute of Standards and Technology Center for Neutron Research; USA); ANSTO (Australian Nuclear Science and Technology Organisation; Australia); J-PARC (Japan Proton Accelerator Research Complex; Japan).

Facility	Instrument	Configuration (E_{res} / μeV)	Q-range (/ $Å^{-1}$)	Accessible time scale	Probed dynamics
ISIS	LET [67]	20.00 μeV (E_i = 1 meV)	0.03–1.32	Sub-ps – Hundreds of ps	(Extremely) Fast dynamics
		500.00 μeV (E_i = 20 meV)	0.14–5.90		
	IRIS [68]	17.50 μeV (PG 002)	0.42–1.85	ps – Hundreds of ps	Intermediate / Fast dynamics
		54.50 μeV (PG 004)	0.84–3.70		
	OSIRIS [69]	25.40 μeV (PG 002)	0.18–1.80	ps – Hundreds of ps	Intermediate / Fast dynamics
		99.00 μeV (PG 004)	0.37–3.60		
ILL	IN16B /BATS [70]	0.75 μeV (Si 111)	0.20–1.80	Tens of ps – ns	Intermediate / Slow dynamics
		2.00 μeV (Si 311)	0.70–3.50		
		1.50 μeV (Si 111)	0.20–1.80		
	SHARP [71]	50.00 μeV (λ = 5.92 Å)	0.20–2.20	Sub-ps – Tens of ps	(Extremely) Fast dynamics
		170.00 μeV (λ = 4.14 Å)	0.20–2.20		
	IN5 [72]	45.00 μeV (λ = 6.00 Å)	0.20–1.60	Sub-ps – Tens of ps	(Extremely) Fast dynamics
		80.00 μeV (λ = 5.00 Å)	0.30–2.50		
FRM-II	TOF-TOF [73]	740.00 μeV (λ = 2.60 Å)	0.40–2.20	Sub-ps – Tens of ps	(Extremely) Fast dynamics
		70.00 μeV (λ = 6.00 Å)	0.20–1.80		
	SPHERES [74]	0.65 μeV (Si 111)	0.20–1.80	Tens of ps – ns	Slow dynamics
PSI	FOCUS [75]	36.00 μeV (λ = 5.75 Å)	0.30–1.80	ps – Hundreds of ps	Intermediate / Fast dynamics
SNS	BASIS [76]	3.50 μeV (Si 111)	0.20–2.00	Tens of ps – ns	Intermediate / Slow dynamics
		15.00 μeV (Si 311)	0.40–3.8		
	CNCS [77]	10.00 μeV (λ = 12.0 Å)	0.10–1.00	ps – Hundreds of ps	Intermediate /
		500.00 μeV (λ = 2.90 Å)	0.40–4.00		Fast dynamics
NIST	HFBS [78]	1.00 μeV (Si 111)	0.10–1.80	Tens of ps – ns	Slow dynamics
	DCS [79]	10.00 μeV (λ = 9.00 Å)	0.10–1.20	ps – Hundreds of ps	Intermediate / Fast dynamics
		500.00 μeV (λ = 2.00 Å)	0.30–6.00		
ANSTO	Emu [80]	1.10 μeV (Si 111)	0.10–1.95	Tens of ps – ns	Intermediate / Slow dynamics
	Pelican [81]	135.00 μeV (λ = 4.69 Å)	0.30–2.20	Sub-ps – ps	(Extremely) Fast dynamics
J-PARC	DNA [82]	1.60 μeV (Si 111)	0.08–1.98	Tens of ps – ns	Slow dynamics
		7.00 μeV (Si 311; in plan)	1.04–3.79		
	AMATERAS [82]	900.00 μeV (E_i = 42 meV)	0.50–7.00	Sub-ps – Tens of ps	Intermediate /(Extremely) Fast dynamics
		10.00 μeV (E_i = 1.7 meV)	0.10–1.50		

I_W are the intermediate scattering functions for polymer and water respectively, and N_{slow} and N_{fast} represent the fraction of "slow" vs "fast" atoms.

In order to obtain additional information about the slower dynamics that are recorded as "immobile" atoms in the initial QENS experiments described above, additional studies must be carried at further spectrometer instrument(s) with higher energy resolution, that can access slower timescales. Typical results for one of our present examples are shown in Fig. 3b. The data from this high resolution spectrometer contains a contribution from the two processes described above (i.e., dynamics extending outside the measurement window, shown as the broad purple curve), plus a new Lorentzian function describing a third and slower dynamical process. This demonstration illustrates how measurements on two or more neutron spectrometers are necessary to obtain QENS data over a full range of timescales necessary to gain a detailed picture of polymer, water and ion dynamics in fuel cell membranes and related systems and devices.

Another effective tool offered by the QENS technique, that resembles a DSC scan in its mode of application and analysis, is the so-called Fixed Window Scan (FWS) measurement. Such a measurement is typically used to locate changes in dynamical behaviour, and it is experimentally obtained by following the evolution of the elastic (EFWS) or inelastic (IFWS) signal as a function of temperature. Moreover, analysis of EFWS data yields the mean square displacement (*msd*) that contains information on both vibrational excitations and proton delocalisation. Analysis of the temperature variation in IFWS provides an estimate of the activation energy (E_A) for those dynamic processes accessible in that specific spectroscopic window (i.e. time scale) [83]. A new experimental set-up that enables simultaneous QENS and DSC measurements has recently been implemented at ISIS to provide complementary information for mapping phase transition temperatures and identifying sample states [84].

5. Examples and case histories

In this section we present two cases involving polymer and side chain dynamics, water relaxation and mobility, and the conduction of cationic or anionic species through the polymer network. These relaxation processes are strongly coupled together over timescales relevant to PEM membranes under operational conditions for FCs and other devices, and we advance that the serial decoupling concept can be usefully applied to disentangle and control the different dynamics, as we seek to design and improve the device efficiency and extend their operating range. We begin with a discussion of Nafion, the industry standard for proton conducting membranes used at current FC operating temperatures, and that has been the subject of multiple studies. Following a discussion of the extensive work carried out to date, we outline how application of the serial decoupling concept can help with further design improvements to the polymer architecture, especially as FC operational temperatures are increased to values beyond the polymer glass transition temperature range (up to 200 °C) [18–20,86–89]. In the second part of this section, we describe on-going work to study and unravel dynamics operating in alkaline fuel cell membranes (AEMFCs). Less is known about these systems which present an additional challenge, AEMs must operate with comparable efficiency in highly alkaline environments [24–28]. Here, recent studies in systems covering a wide range of hydration levels, are applying the serial decoupling concept to disentangle the various dynamical processes and correlate with the anion conductivity.

5.1. Nafion and related proton-conducting membranes

Nafion is the archetypal proton-conducting perfluorosulfonic acid

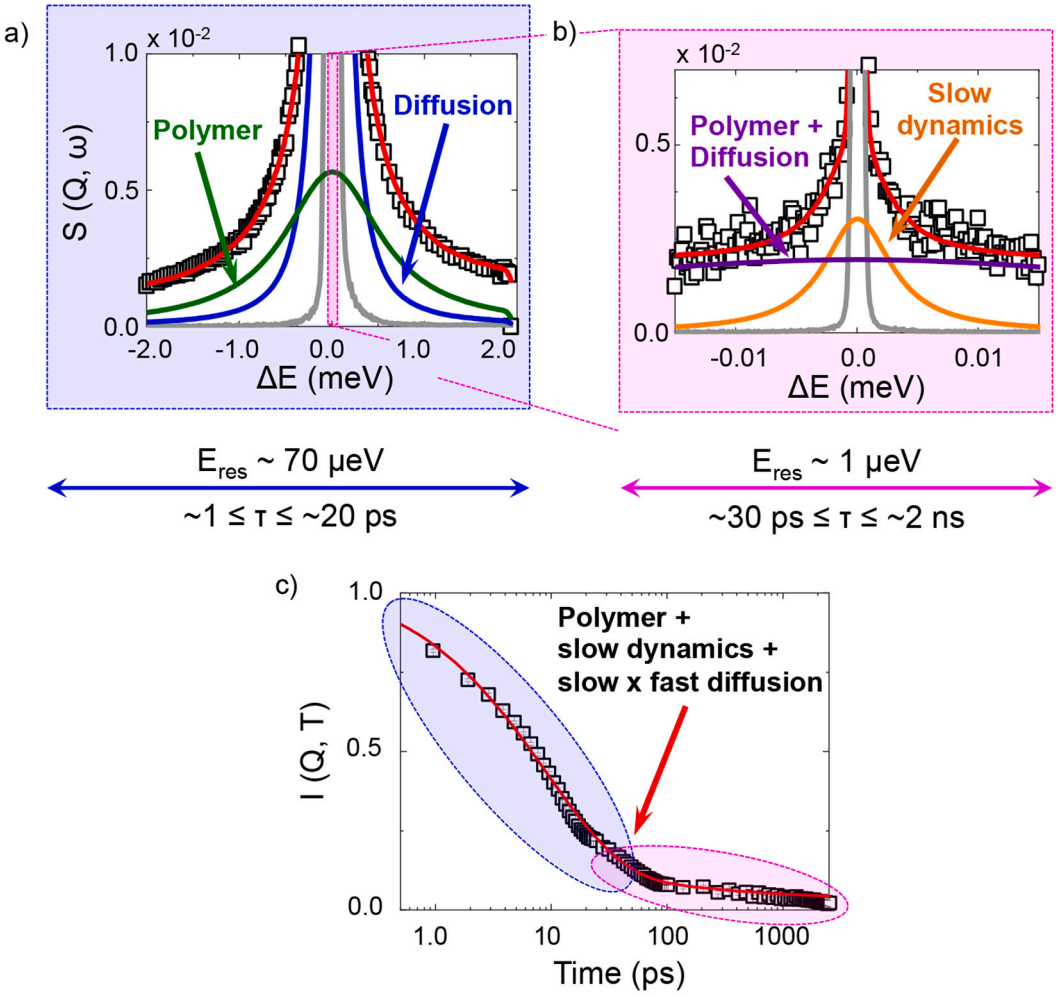

Fig. 3. Comparison between scattering profiles acquired on two neutron spectrometers of different resolutions (namely 70 and 0.75 μeV; IN6-SHARP and IN16B; panel a and b, respectively). The data can be combined as a Fourier transformed function into the time domain to reveal different relaxation dynamics operating sequentially across different timescale ranges (panel c). Adapted from Foglia et al. [85].

(PFSA) membrane used for low temperature fuel cells. Understanding the structure-property relationships in this material (and other PFSAs available from Aquivion, 3 M, Dow membranes, etc.) has been a central focus of extended experimental and numerical studies over several decades [90–91]. The main challenge is to understand the basic mechanisms of proton transport and the impact of multi-scale structure and ion/water dynamics on the global performance, i.e., proton conductivity as a function of polymer and side-chain chemistry, degree of hydration, and operating temperature (Fig. 4).

The amphiphilic nature of Nafion results in nanoscale phase separation where ions, sulfonic acid headgroups and water molecules (Fig. 4a [92]) are located within the interconnected continuous network of ionic domains (Fig. 4b-c [93–96]), which itself is embedded within the hydrophobic matrix composed of ribbon-type aggregates. At larger scales, micron-sized domains give rise to a hierarchical organisation. The main features of such complex multiscale structures (Fig. 4d [96]) have been investigated by small- and wide angle X-ray and neutron scattering techniques, complemented by atomistic (density functional theory, DFT) and nanoscale modelling (including molecular dynamics, MD, and dissipative particle dynamics, DPD). It has been determined that the self-assembled phase-separated morphology directly depends on the local hydration level quantified by $\lambda = [H_2O]/[SO^{3-}]$. The mean size of ionic nanochannels was found to follow a universal swelling law, i.e. independent from the details of polymer backbone carrying perfluorinated side-chains [97]. Accordingly, this parameter appears to directly control the local dynamics (Fig. 4f [60,98]), while large-scale diffusion properties are governed by the macroscopic water content and long-range connectivity (Fig. 4g [53]). Low hydration regions correspond to severe spatial confinement, where water and hydronium ion motions (Figure e [99–100]) deviate from Fickian diffusion [101] and exhibit a sub-diffusive behaviour (i.e. the molecular motions are lengthscale-dependent) (Fig. 4f-g [53,60,101]). This conclusion was established by combining MD, multi-resolution QENS and PFG-NMR performed on PFSA polymers and model ionic surfactants [60]. At high hydration, a bulk-like behaviour is recovered and diffusion becomes obstacle-limited, associated with significant grain boundary and tortuosity effects.

Globally, the multiscale dynamics of water that are key to understand in detail how proton transport mechanisms are balanced depending on the water content, i.e. how structural migration and mass diffusion mechanisms combine to enable efficient long-range transport across the polymer (Fig. 4h-i [100,102–103]). Particularly, the reorganisation of the H-bond network allows the fast charge transfer within Eigen- or Zundel-type clusters, necessitating 2–3 water molecules per ionic group to be effective, while mass diffusion of hydronium ions requires the presence of bulk-like pools of water within ionic domains, e.g. $\lambda > 6$–7. Only a few studies have addressed the relation between solvent dynamics and polymer chain relaxations.

MD simulations [104], neutron spin-echo [105] and NMR [106–107] measurements have indicated that hydration-enhanced polymer chain

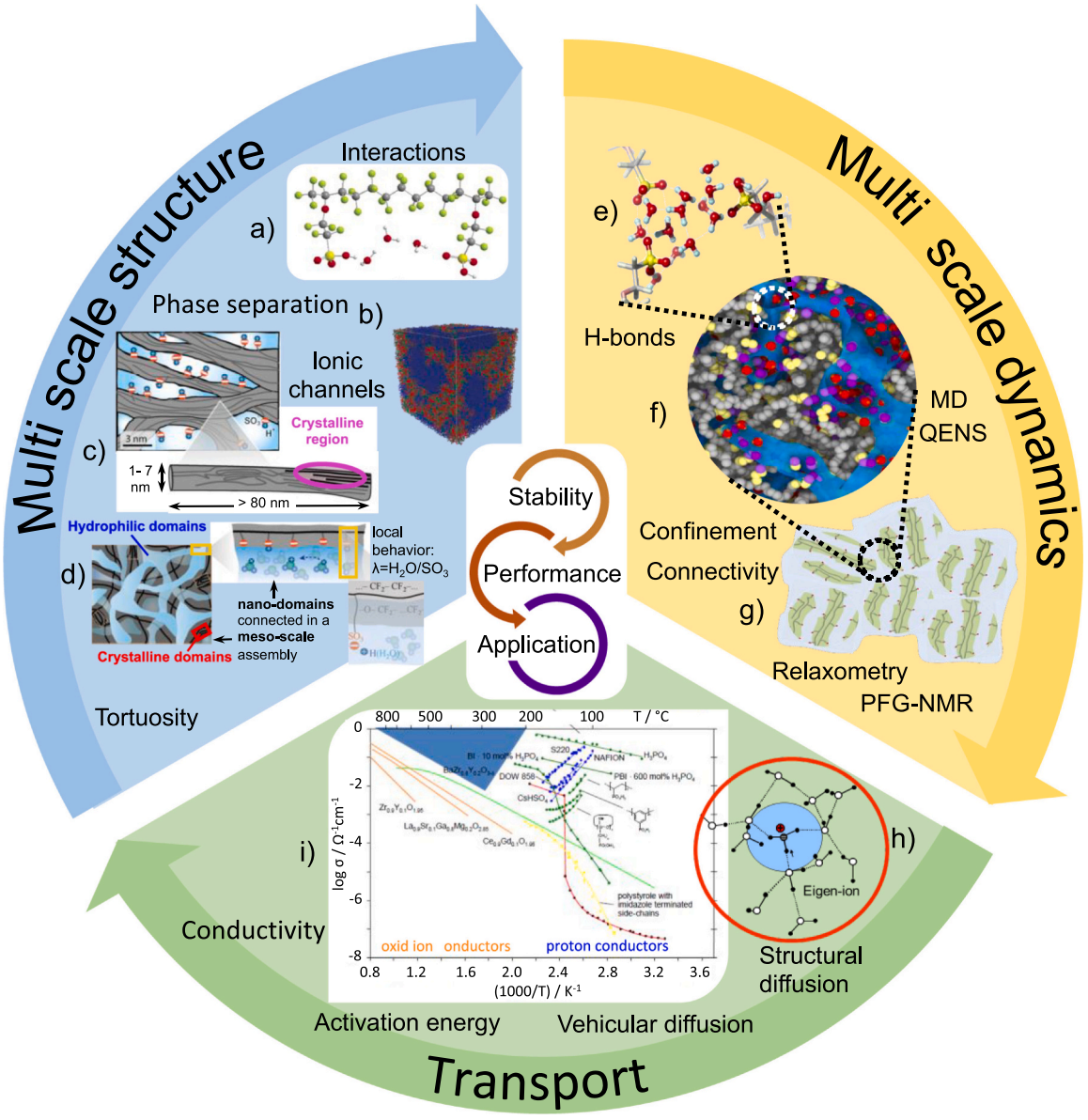

Fig. 4. Structure-property relationship in proton-conducting Nafion membranes. The stability and performance of the polymer in a fuel cell depends primarily on its multiscale structure arising from (a [92]) ionic interactions, (b-c [93–96]) phase-separation at the nanoscale and (d [96]) larger scale hierarchical organisation, and corresponding multiscale ion/water dynamics. The (e [100]) local H-bond network, (f [60]) nanoscale spatial confinement and (g [53,60]) large-scale connectivity all highly depend on the polymer hydration level. At low hydration (high confinement), protons and water molecules exhibit a peculiar sub-diffusive behaviour, which is a universal feature of these systems independent of polymer backbone chemistry, governing the interplay between structural diffusion (h [103]) of protons and mass diffusion of hydronium ions, hence piloting the global ion conductivity (i [14]). Adapted from references [53,60,92–94,96,103].

dynamics may favour fast local ion mobility, although the corresponding relaxation timescales were found to differ by orders of magnitude.

To bypass performance loss that is especially associated with flooding/drying out of the membrane electrode assembly (MEA), major research efforts are now being devoted to the design and development of new systems that can operate at high temperature (HT-PEMFC) and low humidity, while tolerating impure fuel streams. This critical research is expected to lead to PEMFCs that can operate with much higher efficiency, incorporating new membrane systems such as those based on phosphoric-acid-doped polybenzimidazole (PBI) [19,108–110]. These rely on phosphoric acid species embedded within the membrane to enable proton conductivity [111–113]. Current research is directed at optimizing the conductivity and performance of these new membranes via direct modification of the PBI, introducing crosslinkers as well as using additives to reinforce the structure [114–119]. In this scenario of increased structural and dynamic complexity it is essential to implement the ability to understand, deconvolute and control the relationships between intermolecular interactions and cooperative relaxation processes with respect to their relative timescales.

5.2. *Anion-conducting membranes*

Ion conductivity in AEMs is thought to be achieved by a combination of vehicular diffusion and Grotthuss hopping through the water network, with the balance between these two contributing processes determined by the water content (Fig. 5a) [30,32,120–123]. Despite constant improvements in developing higher ion conductivity in AEMFCs, this property still remains considerably lower than in PEMFCs, resulting in a general reluctance to implement these systems that could usefully replace use of Pt-based metal catalysts by less costly and more

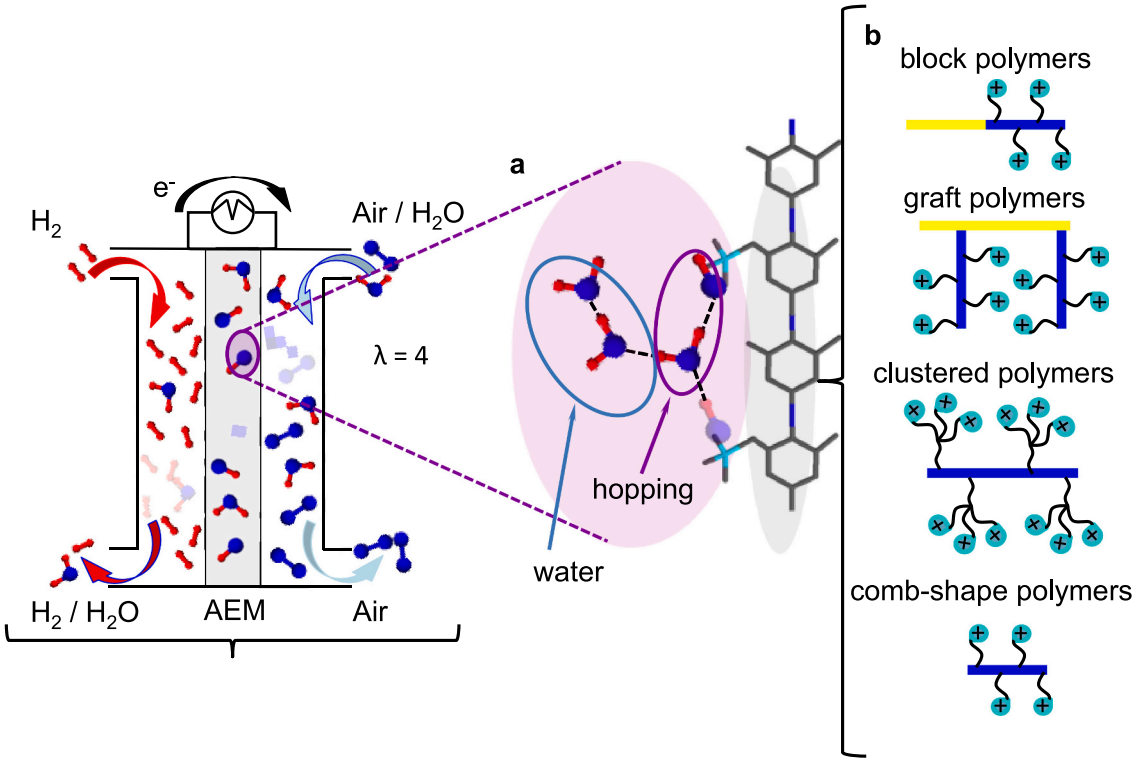

Fig. 5. Schematic illustration of an alkaline fuel cell (AEMFC) and its mode of operation, including a sketch indicating the main modes of OH^-/H_2O transport (panel a [85]) as well as possible polymer architecture (panel b [141]). Adapted from [85 & 141].

sustainable transition metals [24,124]. As for Nafion and other PEMFC systems, optimizing AEM performance requires a deep understanding of the coupling between OH^- hopping and H_2O transport, and how these are modulated by polymer relaxations [125]. This outcome can be achieved by using QENS in combination with other techniques to study the multi-timescale dynamics.

This approach was recently applied to commercial membranes for AEMFC and other applications requiring specific and selective anion conductivity [126–128]. However, the presence of H-containing polymer backbone and functional groups (e.g., quaternary ammonium QA^+ species) used in these materials [129–137] makes the study more complicated, as these dynamics also contribute to the overall scattering profile. Furthermore, the poor thermal and chemical stability of the membrane especially in high pH environments poses a barrier to their operation under temperature conditions especially at low hydration levels, and this has slowed down development of the technology [137]. A further disadvantage is related to the sensitivity of AEMs to carbon dioxide that reacts with OH^- groups to produce (bi)carbonate species, resulting in a reduction in the operating voltage of the cell [138–139]. For this reason, they require a pure fuel stream of H_2 to operate effectively, which considerably raises the operating costs.

With the goal of improving membrane stability and conductance a series of new polymer and side group chemistries along with hybrid mixtures (e.g., by adding SiO_2 and/or TiO_2 to the membrane) have been investigated [140], together with various polymer architectures that have been developed to mimic the phase separation that is important to successful operation of Nafion (Fig. 5b) [141–147]. Besides the classical *comb*-shaped polymer structure, it has been reported that the addition of flexible spacers confers to the membrane a much higher alkaline stability [148], as these enhance the backbone flexibility as well as the formation of ionic clusters, with consequent enhancement of water transport [148–150]. All these chemical/structural modifications further increase the complexity of the system, and it is clear that detailed understanding of the interplay between microscopic physical processes and structure at the macro- to meso-scale, especially under operational conditions, is required to guide the next-generation designs. In this scenario an overall view of sequential (relaxation) processes occurring over a wide time scale (e.g. sub-ps to a few ns) becomes essential. This is possible by following the complex process in the time domain (e.g. *I(Q, t)*; Fig. 3c) where the different processes and the coupling between them are highlighted by their different onset temperatures and relaxation dynamics. This approach then mirrors the "serial decoupling" methodology described by Angell and co-workers.

6. Conclusions

The serial decoupling approach introduced by Angell is a powerful way of evaluating, examining and interpreting the often strongly coupled contributions to the relaxation and diffusional dynamics in molecular glasses and in glass-forming polymers as a function of their characteristic timescale and temperature dependence. It has already proved advantageous in analysing, predicting and optimizing the ionic conductivity of such materials. Here we discuss the wide range of dynamical processes, many coupled together, which are present in ionically conducting polymer membranes designed for use in fuel cells and related applications. Furthermore, we discuss the methods available to study these processes in situ and under operating conditions, with a special emphasis on quasi-elastic neutron scattering that provides simultaneous information on dynamical processes over a wide range of relevant time- and distance scales. We present the current state of knowledge for both proton- and anion-conducting systems, and discuss how the serial decoupling approach could be extended and applied to systematize the different datasets and ultimately help improve membrane performance.

Data availability statement

No new data were created or analysed in this study.

Declaration of Competing Interest

The authors declare that they have no competing interests.

Acknowledgments

FF and PFM have been supported by the EU Graphene Flagship under Horizon 2020 Research and Innovation program Grant Agreement No. 881603- GrapheneCore3, as well as by the EPSRC Materials Research Hub for Energy Conversion, Capture, and Storage (M-RHEX) EP/R023581/1. The authors declare that they have no known competing financial interests or personal relationships that could have appeared to influence the work reported in this paper. The authors declare that they have no competing interests.

References

[1] A.P. Sokolov, V. Garcia Sakai, Experimental techniques for studies of dynamics in soft materials, in: V. Garcia Sakai, C. Albana-Simionescu, S.-A. Chen (Eds.), Dynamics of Soft Matter, Springer USA, 2012, pp. 1–23. ISBN: 978-1-4614-0727-0.
[2] T.E. Gartner III, A. Jayaraman, Modeling and simulations of polymers: a roadmap, Macromolecules 52 (2019) 755–786, https://doi.org/10.1021/acs.macromol.8b01836.
[3] C.A. Angell, Fast ion motion in glassy and amorphous materials, Solid State Ionics 9-10 (1983) 3–16, https://doi.org/10.1016/0167-2738(83)90206-0.
[4] L.M. Torell, C.A. Angell, Ion-matrix coupling in polymer electrolytes from relaxation time studies, British Polymer J. 20 (1988) 173–179, https://doi.org/10.1002/pi.4980200303.
[5] A.L. Agapov, A.P. Sokolov, Decoupling ionic conductivity from structural relaxation: a way to solid polymer electrolytes? Macromolecules 44 (2011) 4410–4414, https://doi.org/10.1021/ma2001096.
[6] D. Bresser, S. Lyonnard, C. Iojoiu, L. Picard, S. Passerini, Decoupling segmental relaxation and ionic conductivity for lithium-ion polymer electrolytes, Mol. Syst. Des. & Eng. 4 (2019) 779–792, https://doi.org/10.1039/c9me00038k.
[7] C.A. Angell, Concepts and conflicts in polymer electrolytes: the search for ion mobility, Electrochim. Acta 313 (2019) 205–219, https://doi.org/10.1016/j.electacta.2019.03.193.
[8] M.A. Hickner, Water-mediated transport in ion-containing polymers, Polymer Physics B 50 (2012) 9–20, https://doi.org/10.1002/polb.22381.
[9] S.B. Aziz, T.J. Woo, M.F.Z. Kadir, H.M. Ahmed, A conceptual review on polymer electrolytes and ion transport models, J. Sci. Adv. Mater. Dev. 3 (2018) 1–17, https://doi.org/10.1016/j.jsamd.2018.01.002.
[10] C.A. Angell, Relaxation in liquids, polymers and plastic crystals - strong/fragile patterns and problems, J. Non-Cryst. Solids 131-133 (1991) 13–31, https://doi.org/10.1016/0022-3093(91)90266-9.
[11] C.A. Angell, Y. Ansari, Z. Zhao, Ionic liquids: past, present and future, Faraday Discuss. 154 (2012) 9–27, https://doi.org/10.1039/c1fd00112d.
[12] K. Ueno, C.A. Angell, On the decoupling of relaxation modes in a molecular liquid caused by isothermal introduction of 2 nm structural inhomogeneities, J. Phys. Chem. B 115 (2011) 13994–13999, https://doi.org/10.1021/jp111398.
[13] C.A. Angell, Ten questions on glassformers, and a real space 'excitations' model with some answers on fragility and phase transitions, J. Phys. Condens. Matter 12 (2000) 6463–6475, https://doi.org/10.1088/0953-8984/12/29/318.
[14] C.A. Angell, K.L. Ngai, G.B. McKenna, P.F. McMillan, S.W. Martin, Relaxation in glassforming liquids and amorphous solids, J. Appl. Phys. 88 (2000) 3113–3157, https://doi.org/10.1063/1.1286035.
[15] A. Brodin, Segmental versus chain dynamics of linear polymers, J. Chem. Phys. 128 (2008), 104901, https://doi.org/10.1063/1.2835603.
[16] S. Mirigian, K.S. Schweizer, Dynamical theory of segmental relaxation and emergent elasticity in supercooled polymer melts, Macromolecules 48 (2015) 1901–1913, https://doi.org/10.1021/ma5022083.
[18] R. Haider, Y. Wen, Z.-F. Ma, D.P. Wilkinson, L. Zhang, X. Yuan, S. Song, J. Zhang, High temperature proton exchange membrane fuel cells: progress in advanced materials and key technologies, Chem. Soc. Rev. 50 (2021) 1138–1187, https://doi.org/10.1039/d0cs00296h.
[19] A. Chandan, M. Hattenberger, A. El-kharouf, S. Du, A. Dhir, V. Self, B.G. Pollet, A. Ingram, W. Bujalski, High temperature (HT) polymer electrolyte membrane fuel cells (PEMFC) - a review, J. Power Sources 231 (2013) 264–278, https://doi.org/10.1016/j.jpowsour.2012.11.126.
[20] V. Atanasov, A.S. Lee, E.J. Park, S. Maurya, E.D. Baca, C. Fujimoto, M. Hibbs, I. Matanovic, J. Kerres, Y.S. Kim, Synergistically integrated phosphonated poly (pentafluorostyrene) for fuel cells, Nat. Mater. 20 (2021) 370–377, https://doi.org/10.1038/s41563-020-00841-z.
[21] H.-Y. Jung, J.W. Kim, Role of the glass transition temperature of Nafion 117 membrane in the preparation of the membrane electrode assembly in a direct methanol fuel cell (DMFC), Int. J. Hydrog. Energy 37 (2012) 12580–12585, 10/1016/j.ijhydene.2012.05.121.
[22] H.R. Corti, F. Nores-Pondal, M.P. Buera, Low temperature thermal properties of Nafion 117 membranes in water and methanol-water mixtures, J. Power Sources 161 (2006) 799–805, https://doi.org/10.1016/j.jpowsour.2006.06.005.
[23] P.W. Majsztrik, A.B. Bocarsly, J.B. Benziger, Viscoelastic response of Nafion. Effects of temperature and hydration on tensile creep, Macromolecules 41 (2008) 9849e, https://doi.org/10.1021/ma801811m.
[24] S. Gottesfeld, D.R. Dekel, M. Page, C. Bae, Y. Yan, P. Zelenay, Y.S. Kim, Anion exchange membrane fuel cells: current status and remaining challenges, J. Power Sources 375 (2018) 170–184, https://doi.org/10.1016/j.jpowsour.2017.08.010.
[25] H. Maša, M. Božič, D. Fakin, K.S. Kleinschek, S. Gorgieva, Alkaline membrane fuel cells: anion exchange membranes and fuels, Sust. Energy Fuels 5 (2021) 604–637, https://doi.org/10.1039/d0se01373k.
[26] M. Hren, M. Božič, D. Fakin, K.S. Kleinschek, S. Gorgieva, Alkaline membrane fuel cells: anion exchange membranes and fuels, Sust. Energy & Fuel 5 (2021) 604–637, https://doi.org/10.1039/D0SE01373K.
[27] W.E. Mustain, M. Chatenet, M. Page, Y.S. Kim, Durability challenges of anion exchange membrane fuel cells, Energy Environ. Sci. 13 (2020) 2805–2838, https://doi.org/10.1039/d0ee01133a.
[28] M. Mandal, G. Huang, N.U. Hassan, X. Peng, T. Gu, A.H. Brooks-Starks, B. Bahar, W.E. Mustain, P.A. Kohl, The importance of water transport in high conductivity and high-power alkaline fuel cells, J. Electrochem. Soc. 167 (2020), 054501, https://doi.org/10.1149/2.0022005JES.
[29] K. Yassin, I.G. Rasin, S. Brandon, D.R. Dekel, Quantifying the critical effect of water diffusivity in anion exchange membranes for fuel cell applications, J. Membr. Sci. 608 (2020), 118206, https://doi.org/10.1016/j.memsci.2020.118206.
[30] V. Dubey, A. Maiti, S. Daschakraborty, Predicting the solvation structure and vehicular diffusion of hydroxide ion in an anion exchange membrane using nonreactive molecular dynamics simulation, Chem. Phys. Lett. 755 (2020), 137802, https://doi.org/10.1016/j.cplett.2020.137802.
[31] T. Zelovich, L. Vogt-Maranto, M.A. Hickner, S.J. Paddison, C. Bae, D.R. Dekel, M. E. Tuckerman, Hydroxide ion diffusion in anion-exchange membranes at low hydration: insights from ab initio molecular dynamics, Chem. Mater. 31 (2019) 5778–5787, https://doi.org/10.1021/acs.chemmater.9b01824.
[32] D. Dong, W. Zhang, A.C.T. van Duin, D. Bedrov, Grotthuss versus vehicular transport of hydroxide in anion-exchange membranes: insight from combined reactive and nonreactive molecular simulations, J. Phys. Chem. Lett. 9 (2018) 825–829, https://doi.org/10.1021/acs.jpclett.8b00004.
[33] E. Çelik, I. Karagöz, Polymer electrolyte membrane fuel cell flow field designs and approaches for performance enhancement, Proceed. Instit. Mech. Eng. Part A 234 (2020) 1189–1214, https://doi.org/10.1177/0957650919893543.
[34] O. Fisette, P. Lagüe, S. Gagné, S. Morin, Synergistic applications of MD and NMR for the study of biological systems, J. Biomed. Biotechnol. 2012 (2011), 254208, https://doi.org/10.1155/2012/254208.
[35] Q. Berrod, K. Lagrené, J. Ollivier, J.-M. Zanotti, Inelastic and quasi-elastic neutron scattering, in: Application to Soft-Matter. *EPJ Web of Conferences* **188**, 2018, p. 05001, https://doi.org/10.1051/epjconf/201818805001.
[36] S. Kmiecik, D. Gront, M. Kolinski, L. Wieteska, A.E. Dawid, A. Kolinski, Coarse-grained protein models and their applications, Chem. Rev. 116 (2016) 7898–7936, https://doi.org/10.1021/acs.chemrev.6b00163.
[37] C.T. Moynihan, A.J. Easteal, J. Wilder, J. Tucker, Dependence of the glass transition temperature on heating and cooling rate, J. Phys. Chem. 78 (1974) 2673–2677, https://doi.org/10.1021/j100619a008.
[38] S. Arrese-Igor, A. Arbe, B. Frick, J. Colmenero, Glassy dynamics of polystyrene by quasielastic neutron scattering, Macromolecules 44 (2011) 3161–3168, https://doi.org/10.1021/ma2001178.
[39] F. Godey, A. Fleury, A. Soldera, Local dynamics within the glass transition domain, Sci. Rep. 9 (2019) 9638, https://doi.org/10.1038/s41598-019-45933-2.
[40] B. Jerome, J. Commandeur, Dynamics of glasses below the glass transition, Nature 386 (1997) 589–592, https://doi.org/10.1038/386589a0.
[41] J.H. Wendorff, The structure of amorphous polymers, Polymer 23 (1982) 543–557, https://doi.org/10.1016/0032-3861(82)90094-5.
[42] R.G. Bryant, The NMR time scale, J. Chem. Educ. 60 (1983) 933–935, https://doi.org/10.1021/ed060p933.
[43] I.R. Kleckner, M.P. Forster, An introduction to NMR-based approaches for measuring protein dynamics, Biochim. Biophys. Acta 2011 (1814) 942–968, https://doi.org/10.1016/j.bbapap.2010.10.012.
[44] J. Zhang, M.V. Giotto, W.-Y. Wen, A.A. Jones, An NMR study of the state of ions and diffusion in perfluorosulfonate ionomer, J. Membr. Sci. 269 (2006) 118–125, https://doi.org/10.1016/j.memsci.2005.06.026.
[45] X. Yan, G. He, X.Wu.J. Benziger, Ion and water transport in functionalized PEEK membranes, Journal of Membrane Science 429 (2013) 13–22, https://doi.org/10.1016/j.memsci.2012.11.026.
[46] M.G. Marino, J.P. Melchior, A. Wohlfarth, K.D. Kreuer, Hydroxide, halide and water transport in a model anion exchange membrane, J. Membr. Sci. 464 (2014) 61–71, https://doi.org/10.1016/j.memsci.2014.04.003.
[47] E. Galitskaya, A.F. Privalov, M. Weigler, M. Vogel, A. Kashin, M. Ryzhkin, V. Sinitsyn, NMR diffusion studies of proton-exchange membranes in wide temperature range, J. Membr. Sci. 596 (2020), 117691, https://doi.org/10.1016/j.memsci.2019.117691.
[48] J. Kärger, M. Avramovska, D. Freude, J. Haase, S. Hwang, R. Valiullin, Pulsed field gradient NMR diffusion measurement in nanoporous materials, Adsorption 27 (2021) 453–484, https://doi.org/10.1007/s10450-020-00290-9.
[49] P.T. Callaghan, Pulsed field gradient nuclear magnetic resonance as a probe of liquid state molecular organization, Aust. J. Phys. 37 (1984) 359–387, https://doi.org/10.1071/PH840539.
[50] P.T. Callaghan, S.L. Codd, J.D. Seymour, Spatial coherence phenomena arising from translational spin motion in gradient spin echo experiments, Conc Mag. Res.

11 (1999) 181–202, https://doi.org/10.1002/(SICI)1099-0534(1999)11:4<181::AID-CMR1>3.0.CO;2-T.
[51] P.T. Callaghan, D.N. Pinder, A pulsed field gradient NMR study of self-diffusion in a polydisperse polymer system: dextran in water, Macromolecules 16 (1983) 968–973, https://doi.org/10.1021/ma00240a028.
[52] J.-C. Perrin, S. Lyonnard, A. Guillermo, P. Levitz, Water dynamics in ionomer membranes by field-cycling NMR relaxometry, J. Phys. Chem. B 110 (2006) 5439–5444, https://doi.org/10.1021/jp057433e.
[53] J.-C. Perrin, S. Lyonnard, A. Guillermo, P. Levitz, Water dynamics in Ionomer membranes by field-cycling NMR relaxometry, Fuel Cells 6 (2006) 5–9, https://doi.org/10.1002/fuce.200500094.
[54] J.-C. Perrin, S. Lyonnard, A. Guillermo, P. Levitz, Water dynamics in ionomer membranes by field-cycling NMR relaxometry, Magn. Reson. Imaging 25 (2007) 501–504, https://doi.org/10.1016/j.mri.2007.01.002 (PMID: 17466773).
[55] S. Tsushima, K. Teranishi, K. Nishida, S. Hirai, Water content distribution in a polymer electrolyte membrane for advanced fuel cell system with liquid water supply, Magn. Reson. Imaging 23 (2005) 255–258, https://doi.org/10.1016/j.mri.2004.11.059.
[56] Z. Zhang, J. Martin, J. Wu, H. Wang, K. Promlislow, B.J. Balcom, Magnetic resonance imaging of water content across the Nafion membrane in an operational PEM fuel cell, J. Magn. Reson. 193 (2008) 259–266, https://doi.org/10.1016/j.jmr.2008.05.005.
[57] S. Schumann, J.W. Simkins, N. Schork, S.L. Codd, J.D. Seymour, M. Heijnen, F. Saravia, H. Horn, N. Nirschi, G. Guthausen, Characterization and quantification of structure and flow in multichannel polymer membranes by MRI, J. Membr. Sci. 570-571 (2019) 472–480, https://doi.org/10.1016/j.memsci.2018.10.072.
[58] M. Bee, Quasielastic Neutron Scattering, Adam Hilger, Bristol, 1988. ISBN: 978–0852743713.
[59] M.T.F. Telling, A Practical Guide to Quasi-Elastic Neutron Scattering (2020), Royal Society of Chemistry, 2021. ISBN: 9781788012621.
[60] Q. Berrod, S. Hanot, A. Guillermo, S. Mossa, S. Lyonnard, Water sub-diffusion in membranes for fuel cells, Sci. Rep. 7 (2017) 8326, https://doi.org/10.1038/s41598-017-08746-9.
[61] J.-P. Melchior, B. Frick, On the nanosecond proton dynamics in phosphoric acid-benzimidazole and phosphoric acid-water mixtures, Phys. Chem. Chem. Phys. 19 (2017) 28540, https://doi.org/10.1039/c7cp04116k.
[62] H. Paoli, A. Methivier, H. Jobic, C. Krause, H. Pfeifer, F. Stallmach, J. Kärger, Comparative QENS and PFG NMR diffusion studies of water in zeolite NaCaA, Microporous Mesoporous Mater. 55 (2002) 147–158, https://doi.org/10.1016/S1387-1811(02)00399-2.
[63] T.R. Graham, D. Semrouni, E. Mamontov, A.J. Ramirez-Cuesta, K. Page, A. Clark, G.K. Schenter, C.I. Pearce, A.G. Stack, H.-W. Wang, Coupled multimodal dynamics of hydrogen-containing ion networks in water-deficient, sodium hydroxide-aluminate solutions, J. Phys. Chem. B 122 (2018) 12097–12106, https://doi.org/10.1021/acs.jpcb.8b09375.
[64] M.C. Bellissent-Funel, S.H. Chen, J.-M. Zanotti, Single-particle dynamics of water molecules in confined space, Phys. Rev. E 51 (1995) 4558–4569, https://doi.org/10.1103/physreve.51.4558.
[65] F. Volino, A. Dianoux, Neutron incoherent scattering law for diffusion in a potential of spherical symmetry: general formalism and application to diffusion inside a sphere, Mol. Phys. 41 (1980) 271–279, https://doi.org/10.1080/00268978000102761.
[66] J.-C. Perrin, S. Lyonnard, F. Volino, Quasielastic neutron scattering study of water dynamics in hydrated nafion membranes, J. Phys. Chem. C 111 (2007) 3393–3404, https://doi.org/10.1021/jp065039q.
[67] ISIS, Let. https://www.isis.stfc.ac.uk/Pages/Let-technical-information.aspx, 2021.
[68] ISIS, Iris. https://www.isis.stfc.ac.uk/Pages/Iris-technical-information.aspx, 2021.
[69] ISIS, Osiris. https://www.isis.stfc.ac.uk/Pages/Osiris-technical-information.aspx, 2021.
[70] ILL, In16b. https://www.ill.eu/users/instruments/instruments-list/in16b/characteristics, 2021.
[71] ILL, Sharp. https://www.ill.eu/users/instruments/instruments-list/sharp/characteristics, 2021.
[72] ILL, In5. https://www.ill.eu/users/instruments/instruments-list/in5/characteristics, 2021.
[73] FRM-II, TofTof. https://mlz-garching.de/toftof, 2021.
[74] FRM-II, Spheres. https://mlz-garching.de/spheres, 2021.
[75] PSI, Focus. https://www.psi.ch/en/sinq/focus, 2021.
[76] SNS, Basis. https://neutrons.ornl.gov/basis, 2021.
[77] SNS, Cncs. https://neutrons.ornl.gov/cncs, 2021.
[78] NIST, Hfbs. https://www.nist.gov/ncnr/hfbs-instrument-details, 2021.
[79] NIST, Dcs. https://www.nist.gov/ncnr/dcs-design-features-and-principal-specifications, 2021.
[80] ANSTO, Emu. https://www.ansto.gov.au/technical-information-emu, 2021.
[81] ANSTO, Pelican. https://www.ansto.gov.au/user-access/instruments/neutron-scattering-instruments/pelican-time-of-flight-spectrometer-0, 2021.
[82] J-Parc, Dna & Amateras. https://j-parc.jp/researcher/MatLife/en/instrumentation/ns_spec.html, 2021.
[83] B. Frick, J. Combet, L. van Eijck, New possibilities with inelastic fixed window scans and linear motor Doppler drives on high resolution neutron backscattering spectrometers, in: Nuclear Instruments and Methods in Physics Research Section A: Accelerators Spectrometers Detectors and Associated Equipment 669, 2012, pp. 7–13, https://doi.org/10.1016/j.nima.2011.11.090.
[84] D. Fornalski, V. García Sakai, S. Postorino, I. Silverwood, C. Goodway, J. Bones, O. Kirichek, F. Fernandez-Alonso, Simultaneous thermodynamic and dynamical characterisation using *in situ* calorimetry with neutron spectroscopy, Low Temp. Phys. 45 (2019) 289–293, https://doi.org/10.1063/1.5090042.
[85] F. Foglia, S. Lyonnard, V. García Sakai, Q. Berrod, J.-M. Zanotti, G. Gebel, A. J. Clancy, P.F. McMillan, Progress in neutron techniques: towards improved polymer electrolyte membranes for energy devices, J. Phys. Condens. Matter 33 (2021), 264005, https://doi.org/10.1088/1361-648X/abfc10.
[86] A. Ignaszak, C. Song, W. Zhu, J. Zhang, A. Bauer, R. Baker, V. Neburchilov, S. Ye, S. Campbell, Titanium carbide and its core-shelled derivative TiC@TiO2 as catalyst supports for proton exchange membrane fuel cells, Electrochim. Acta 69 (2012) 397–405, https://doi.org/10.1016/j.electacta.2012.03.039.
[87] J. Jalili, M. Geppi, V. Tricoli, Organic protic ionics based on Nitrilo (trimethylenephosphonic acid) as water-free, proton-conducting materials, J. Solid State Electrochem. 19 (2015) 1643–1650, https://doi.org/10.1007/s10008-015-2792-0.
[88] H. Saidi, H. Uthman, Phosphoric acid doped polymer electrolyte membrane based on radiation grafted poly(1-vinylimidazole-co-1-vinyl-2-pyrrolidone)-g-poly (ethylene/tetrafluoroethylene) copolymer and investigation of grafting kinetics, Int. J. Hydrog. Energy 42 (2017) 9315–9332, https://doi.org/10.1016/j.ijhydene.2016.06.187.
[89] F. Mack, S. Galbiati, V. Gogel, L. Jörissen, R. Zeis, Evaluation of electrolyte additives for high-temperature polymer electrolyte fuel cells, ChemElectroChem 3 (2016) 770–773, https://doi.org/10.1002/celc.201500561.
[90] A. Kusoglu, A.Z. Weber, New insights into perfluorinated sulfonic-acid ionomers, Chem. Rev. 117 (2017) 987–1104, https://doi.org/10.1021/acs.chemrev.6b00159.
[91] S. Lyonnard, G. Gebel, Neutrons for fuel cell membranes: Structure, sorption and transport properties, The Eur. Phys. J. Special Top. 213 (2012) 195–211, https://doi.org/10.1140/epjst/e2012-01671-6.
[92] S.J. Paddison, J.A. Elliott, Molecular modeling of the short-side-chain perfluorosulfonic acid membrane, J. Phys. Chem. A 109 (2005) 7583–7593, https://doi.org/10.1021/jp0524734.
[93] D. Wu, S.J. Paddison, J.A. Elliott, Effect of molecular weight on hydrated morphologies of the short-side-chain perfluorosulfonic acid membrane, Macromolecules 42 (2009) 3358–3367, https://doi.org/10.1021/ma900016w.
[94] L. Rubatat, G. Gebel, O. Diat, Fibrillar structure of nafion:matching fourier and real space studies of corresponding films and solutions, Macromolecules 37 (2004) 7772–7783, https://doi.org/10.1021/ma049683j.
[95] K.-D. Kreuer, G. Portale, A critical revision of the nano-morphology of proton conducting ionomers and polyelectrolytes for fuel cell applications, Adv. Funct. Mater. 23 (2013) 5390–5397, https://doi.org/10.1002/adfm.201300376.
[96] A. Kusoglu, A.Z. Weber, New insights into perfluorinated sulfonic-acid ionomers, Chem. Rev. 117 (2017) 987–1104, https://doi.org/10.1021/acs.chemrev.6b00159.
[97] H.-D. Nguyen, L. Assumma, P. Judeinstein, R. Mercier, L. Porcar, J. Jestin, C. Iojoiu, S. Lyonnard, Controlling microstructure–transport interplay in highly phase-separated perfluorosulfonated aromatic multiblock ionomers via molecular architecture design, ACS Appl. Mater. Interfaces 9 (2017) 1671–1683, https://doi.org/10.1021/acsami.6b12764.
[98] Q. Berrod, S. Lyonnard, A. Guillermo, J. Ollivier, B. Frick, G. Gébel, QENS investigation of proton confined motions in hydrated perfluorinated sulfonic membranes and self-assembled surfactants, EPJ Web Conf. 83 (2015) 02002, https://doi.org/10.1051/epjconf/20158302002.
[99] S. Dalla Bernardina, J.B. Brubach, Q. Berrod, A. Guillermo, P. Judeinstein, P. Roy, S. Lyonnard, Mechanism of ionization, hydration, and intermolecular H-bonding in proton conducting nanostructured ionomers, J. Phys. Chem. C 118 (2014) 25468–25479, https://doi.org/10.1021/jp5074818.
[100] S. Lyonnard, Q. Berrod, B.-A. Brüning, G. Gebel, A. Guillermo, H. Ftouni, J. Ollivier, B. Frick, Perfluorinated surfactants as model charged systems for understanding the effect of confinement on proton transport and water mobility in fuel cell membranes. A study by QENS, Eur. Phys. J. Special Top. 189 (2010) 205–216, https://doi.org/10.1140/epjst/e2010-01324-x.
[101] S. Hanot, S. Lyonnard, S. Mossa, Sub-diffusion and population dynamics of water confined in soft environments, Nanoscale 8 (2016) 3314–3325, https://doi.org/10.1039/c5nr05853h.
[102] K.D. Kreuer, S.J. Paddison, E. Spohr, M. Schuster, Transport in proton conductors for fuel-cell applications: simulations, elementary reactions, and phenomenology, Chem. Rev. 104 (2004) 4637–4678, https://doi.org/10.1021/cr020715f.
[103] K.D. Kreuer, On the complexity of proton conduction phenomena, Solid State Ionics 136 (2000) 149–160, https://doi.org/10.1016/S0167-2738(00)00301-5.
[104] H. Liu, S. Cavaliere, D.J. Jones, J. Rozière, S.J. Paddison, Scaling behavior of nafion with different model parameterizations in dissipative particle dynamics simulations, Macromol. Theor Simulat. 27 (2018) 1800003, https://doi.org/10.1002/mats.201800003.
[105] K.A. Page, B.W. Rowe, K.A. Masser, A. Faraone, The effect of water content on chain dynamics in nafion membranes measured by neutron spin echo and dielectric spectroscopy, J. Polym. Sci. B Polym. Phys. 52 (2014) 624–632, https://doi.org/10.1002/polb.23457.
[106] K.A. Page, K.M. Cable, R.B. Moore, Molecular origins of the thermal transitions and dynamic mechanical relaxations in perfluorosulfonate ionomers, Macromolecules 38 (2005) 6472–6484, https://doi.org/10.1021/ma0503559.
[107] Q. Chen, K. Schmidt-Rohr, Backbone dynamics of the nafion ionomer studied by 19F-13C solid-state NMR, Macromol. Chem. Phys. 208 (2007) 2189–2203, https://doi.org/10.1002/macp.200700200.

[108] K.-D. Kreuer, Ion conducting membranes for fuel cells and other electrochemical devices, Chem. Mater. 26 (2014) 361–380, https://doi.org/10.1021/cm402742u.
[109] H. Steininger, M. Schuster, K.D. Kreuer, A. Kaltbeitzel, B. Bingöl, W.H. Meyer, S. Schauff, G. Brunklaus, J. Maier, H.W. Spiess, Intermediate temperature proton conductors for PEM fuel cells based on phosphonic acid as protogenic group: a progress report, Phys. Chem. Chem. Phys. 9 (2007) 1764–1773, https://doi.org/10.1039/B618686F.
[110] H. Vogel, C.S. Marvel, Polybenzimidazoles, new thermally stable polymers, J. Polym. Sci. 50 (1961) 511–539, https://doi.org/10.1002/pol.1961.1205015419.
[111] J.S. Wainright, J.-T. Wang, D. Weng, R.F. Savinell, M. Litt, Acid-doped polybenzimidazoles: a new polymer electrolyte, J. Electrochem. Soc. 142 (1995) L121, https://doi.org/10.1149/1.2044337.
[112] J.-T. Wang, R.F. Savinell, J. Wainright, M. Litt, H. Yu, A fuel cell using acid doped polybenzimidazole as polymer electrolyte, Electrochim. Acta 41 (1996) 193–197, https://doi.org/10.1016/0013-4686(95)00313-4.
[113] H. Bai, Y. Li, H. Zhang, H. Chen, W. Wu, J. Wang, J. Liu, Anhydrous proton exchange membranes comprising of chitosan and phosphorylated graphene oxide for elevated temperature fuel cells, J. Membr. Sci. 495 (2015) 48–60, https://doi.org/10.1016/j.memsci.2015.08.012.
[114] S. Wang, C. Zhao, W. Ma, N. Zhang, Y. Zhang, G. Zhang, Z. Liu, H. Na, Silanecross-linked polybenzimidazole with improved conductivity for high temperature proton exchange membrane fuel cells, J. Mater. Chem. A 1 (2013) 621–629, https://doi.org/10.1039/C2TA00216G.
[115] J. Yang, D. Aili, Q. Li, L.N. Cleemann, J.O. Jensen, N.J. Bjerrum, R. He, Covalently cross-linked sulphone polybenzimidazole membranes with poly(vinylbenzyl chloride) for fuel cell applications, ChemSusChem 6 (2013) 275–282, https://doi.org/10.1002/cssc.201200716.
[116] S. Wang, G. Zhang, M. Han, H. Li, Z. Yang, J. Ni, W. Ma, M. Li, J. Wang, Z. Liu, L. Zhang, H. Na, Novel epoxy-based cross-linked polybenzimidazole for high temperature proton exchange membrane fuel cells, Int. J. Hydrog. Energy 36 (2011) P8412–P8421, https://doi.org/10.1016/j.ijhydene.2011.03.147.
[117] Q. Li, H.C. Rudbeck, A. Chromik, J. Jensen, C. Pan, T. Steenberg, M. Calverley, N. Bjerrum, J. Kerres, Properties degradation and high temperature fuel cell test of different types of PBI and PBI blend membranes, J. Membr. Sci. 347 (2010) 260–270, https://doi.org/10.1016/J.MEMSCI.2009.10.032.
[118] H.-Y. Li, Y.-L. Liu, Polyelectrolyte composite membranes of polybenzimidazole and crosslinked polybenzimidazole polybenzoxazine electrospun nanofibers for proton exchange membrane fuel cells, J. Mater. Chem. A 1 (2013) 1171–1178, https://doi.org/10.1039/c2ta00270a.
[119] R. Harilal, P.C. Ghosh Nayak, T. Jana, Cross-linked polybenzimidazole membrane for PEM fuel cells, ACS Appl. Polymer Mater. 2 (2020) 3161–3170. https://pubs.acs.org/doi/10.1021/acsapm.0c00350.
[120] D. Marx, A. Chandra, M.E. Tuckerman, Aqueous basic solutions: hydroxide solvation, structural diffusion, and ccomparison to the hydrated proton, Chem. Rev. 110 (2010) 2174–2216, https://doi.org/10.1021/cr900233f.
[121] M.E. Tuckerman, D. Marx, M. Parrinello, The nature and transport mechanism of hydrated hydroxide ions in aqueous solution, Nature 417 (2002) 925–929, https://doi.org/10.1038/nature00797.
[122] C. Chen, Y.-L.S. Tse, G.E. Lindberg, C. Knight, G.A. Voth, Hydroxide solvation and transport in anion exchange membranes, J. Am. Chem. Soc. 138 (2016) 991–1000, https://doi.org/10.1021/jacs.5b11951.
[123] W. Zhang, D. Dong, D. Bedrov, A.C.T. van Duin, Hydroxide transport and chemical degradation in anion exchange membranes: a combined reactive and non-reactive molecular simulation study, J. Mater. Chem. A 7 (2019) 5442–5452, https://doi.org/10.1039/c8ta10651g.
[124] S. Subianto, M. Pica, M. Casciola, P. Cojocaru, L. Merlo, G. Hards, D.J. Jones, Physical and chemical modification routes leading to improved mechanical properties of perfluorosulfonic acid membranes for PEM fuel cells, J. Power Sources 233 (2013) 216–230, https://doi.org/10.1016/j.jpowsour.2012.12.121.
[125] N. Martinez, A. Morin, Q. Berrod, B. Frick, J. Ollivier, L. Porcar, G. Gebel, S. Lyonnard, Multiscale water dynamics in a fuel cell by operando quasi elastic neutron scattering, J. Phys. Chem. C 122 (2018) 1103–1108, https://doi.org/10.1021/acs.jpcc.7b11189.
[126] F. Foglia, Q. Berrod, A.J. Clancy, K. Smith, G. Gebel, V. García Sakai, M. Appel, J.-M. Zanotti, M. Tyagi, N. Mahmoudi, T.S. Miller, J.R. Varcoe, A. Periasamy, D.J. L. Brett, P.R. Shearing, S. Lyonnard, P.F. McMillan, Disentangling water, ion and polymer dynamics in an anion exchange membrane, Nat. Mater. (2021) (in revision).
[127] J.-P. Melchior, W. Lohstroh, M. Zamponni, N.H. Jalarvo, Multiscale water dynamics in model anion exchange membranes for alkaline membrane fuel cells, J. Membr. Sci. 586 (2019) 240–247, https://doi.org/10.1016/j.memsci.2019.05.079.
[128] J.-P. Melchior, N.H. Jalarvo, A quasielastic neutron scattering study of water diffusion in model anion exchange membranes over localized and extended volume increments, J. Phys. Chem. C 123 (2019) 14195–14206, https://doi.org/10.1021/acs.jpcc.9b01873.
[129] J. Yan, M.A. Hickner, Anion exchange membranes by bromination of benzylmethyl-containing poly(sulfone)s, Macromolecules 43 (2010) 2349–2356, https://doi.org/10.1021/ma902430y.
[130] M.R. Hibbs, M.A. Hickner, T.M. Alam, S.K. McIntyre, C.H. Fujimoto, C. J. Cornelius, Transport properties of hydroxide and proton conducting membranes, Chem. Mater. 20 (92008) (2021) 2566–2573, https://doi.org/10.1021/cm703263n.
[131] E.E. Switzer, T.S. Olson, A.K. Datye, P. Atanassov, M.R. Hibbs, C. Fujimoto, C. J. Cornelius, Novel KOH-free anion-exchange membrane fuel cell: performance comparison of alternative anion-exchange ionomers in catalyst ink, Electrochim. Acta 55 (2010) 3404–3408, https://doi.org/10.1016/j.electacta.2009.12.073.
[132] J.R. Varcoe, Investigations of the ex situ ionic conductivities at 30 deg C of metal-cation-free quaternary ammonium alkaline anion-exchange membranes in static atmospheres of different relative humidities, Phys. Chem. Chem. Phys. 9 (2007) 1479–1486, https://doi.org/10.1039/B615478F.
[133] L. Wang, X. Peng, W.E. Mustain, J.R. Varcoe, Radiation-grafted anion-exchange membranes: the switch from low- to high-density polyethylene leads to remarkably enhanced fuel cell performance, Energy Environ. Sci. 12 (2019) 1575–1579, https://doi.org/10.1039/C9EE00331B.
[134] J.Y. Jeon, S. Park, J. Han, S. Maurya, A.D. Mohanty, D. Tian, N. Saikia, M. A. Hickner, C.Y. Ryu, M.E. Tuckerman, S.J. Paddison, Y.S. Kim, C. Bae, Synthesis of aromatic anion exchange membranes by Friedel-crafts bromoalkylation and cross-linking of polystyrene block copolymers, Macromolecules 52 (2019) 2139–2147, https://doi.org/10.1021/acs.macromol.8b02355.
[135] J. Pan, J. Han, L. Zhu, M.A. Hickner, Cationic side-chain attachment to poly (phenylene oxide) backbones for chemically stable and conductive anion exchange membranes, Chem. Mater. 29 (2017) 5321–5330, https://doi.org/10.1021/acs.chemmater.7b01494.
[136] X. Liao, L. Ren, D. Chen, X. Liu, H. Zhang, Nanocomposite membranes based on quaternized polysulfone and functionalized montmorillonite for anion-exchange membranes, J. Power Sources 286 (2015) 258–263, https://doi.org/10.1016/j.jpowsour.2015.03.182.
[137] N. Ramaswamy, S. Mukerjee, Alkaline anion-exchange membrane fuel cells: challenges in electrocatalysis and interfacial charge transfer, Chem. Rev. 119 (2019) 11945–11979, https://doi.org/10.1021/acs.chemrev.9b00157.
[138] N. Ziv, W.E. Mustain, D.R. Dekel, The effect of ambient carbon dioxide on anion-exchange membrane fuel cells, ChemSusChem 11 (2018) 1136–1150, https://doi.org/10.1002/cssc.201702330.
[139] Y. Zheng, L.N.I. Colón, N.U. Hassan, E.R. Williams, M. Stefik, J.M. LaManna, D. S. Hussey, W.E. Mustain, Effect of membrane properties on the carbonation of anion exchange membrane fuel cells, Membranes 11 (2021) 102, https://doi.org/10.3390/membranes11020102.
[140] S. Castañeda Ramírez, R. Ribadeneira Paz, Hydroxide transport in anion-exchange membranes for alkaline fuel cells, in: New Trends in Ion Exchange Studies, 2018, pp. 51–70. Edited by S. Karakuş. IntechOpen. ISBN: 978-1-78984-248-7.
[141] F. Xu, Y. Su, B. Lin, Progress of alkaline anion exchange membranes for fuel cells: the effects of micro-phase separation, Front. Mater. 7 (2020) 4, https://doi.org/10.3389/fmats.2020.00004.
[142] M. Tanaka, K. Fukasawa, E. Nishino, S. Yamaguchi, K. Yamada, H. Tanaka, B. Bae, K. Miyatake, M. Watanabe, Anion conductive block poly(arylene ether)s: synthesis, properties, and application in alkaline fuel cells, J. Am. Chem. Soc. 133 (2011) 10646–10654, https://doi.org/10.1021/ja204166e.
[143] L. Liu, D.F. Li, Y. Xing, N.W. Li, Mid-block quaternized polystyrene- b-polybutadiene-b-polystyrene triblock copolymers as anion exchange membranes, J. Membr. Sci. 564 (2018) 428–435, https://doi.org/10.1016/j.memsci.2018.07.055.
[144] B. Lin, F. Xu, Y. Su, Z. Zhu, Y. Ren, J. Ding, N. Yuan, Facile preparation of anion exchange membrane based on polystyreneb- polybutadiene-b-polystyrene for the application of alkaline fuel cells, Ind. Eng. Chem. Res. 58 (2019) 22299–22305, https://doi.org/10.1021/acs.iecr.9b05314.
[145] J.R. Varcoe, R.C.T. Slade, E.L.H. Yee, S.D. Poynton, D.J. Driscoll, D.C. Apperley, Poly(ethylene-co-tetrafluoroethylene)- derived radiation-grafted anion-exchange membrane with properties specifically tailored for application in metal-cation-free alkaline polymer electrolyte fuel cells, Chem. Mater. 19 (2007) 2686–2693, https://doi.org/10.1021/cm0 62407u.
[146] L. Zhu, J. Pan, Y. Wang, J. Han, L. Zhuang, M.A. Hickner, Multication side chain anion exchange membranes, Macromolecules 49 (2016) 815–824, https://doi.org/10.1021/acs.macromol.5b02671.
[147] N. Li, Y. Leng, M.A. Hickner, C.-Y. Wang, Highly stable, anion conductive, combshaped copolymers for alkaline fuel cells, J. Am. Chem. Soc. 135 (2013) 10124–10133, https://doi.org/10.1021/ja403671u.
[148] H.S. Dang, P. Jannasch, Exploring different cationic alkyl side chain designs for enhanced alkaline stability and hydroxide ion conductivity of anion-exchange membranes, Macromolecules 48 (2015) 5742–5751, https://doi.org/10.1021/acs.macromol.5b01302.
[149] D.R. Dekel, I.R. Rasin, S. Brandon, Predicting performance stability of anion exchange membrane fuel cells, J. Power Sources 420 (2019) 118–123, https://doi.org/10.1016/j.jpowsour.2019.02.069.
[150] M.R. Hibbs, Alkaline stability of poly (phenylene)-based anion exchange membranes with various cations, J. Polym. Sci. B Polym. Phys. 51 (2013) 1736–1742, https://doi.org/10.1002/polb.23149.